Topological defects in mixtures of superconducting condensates with different charges

Julien Garaud[1,2,*] and Egor Babaev[1,2]

[1]*Department of Physics, University of Massachusetts, Amherst, Massachusetts 01003, USA*

[2]*Department of Theoretical Physics, Royal Institute of Technology, Stockholm SE-10691, Sweden*

(Received 14 March 2014; revised manuscript received 30 May 2014; published 18 June 2014)

We investigate the topological defects in phenomenological models describing mixtures of charged condensates with commensurate electric charges. Such situations are expected to appear for example in liquid metallic deuterium. This is modeled by a multicomponent Ginzburg-Landau theory where the condensates are coupled to the same gauge field by different coupling constants whose ratio is a rational number. We also briefly discuss the case where electric charges are incommensurate. Flux quantization and finiteness of the energy per unit length dictate that the different condensates have different winding and thus different number of (fractional) vortices. Competing attractive and repulsive interactions lead to molecule-like bound states between fractional vortices. Such bound states have finite energy and carry integer flux quanta. These can be characterized by the $\mathbb{C}P^1$ topological invariant that motivates their denomination as skyrmions.

DOI: 10.1103/PhysRevB.89.214507 PACS number(s): 67.85.Jk, 74.25.Ha, 67.85.Fg

I. INTRODUCTION

Although recently there has been substantial interest in multicomponent superconductors, typically the research is restricted to fields which have the same value of electric charge modulus. See, e.g., Ref. [1] for recent work with a field overview. In the typical condensed matter systems the charge is set by a Cooper pair charge of $2e$ for electronic systems or $-2e$ for protonic superconductors [2,3]. By contrast, multicomponent systems with different values of electric charge attracted much less attention, yet some were discussed in the literature. One example is liquid metallic deuterium where the deuteron is a charge-1 boson which can Bose condense and coexist with the Cooper pairs of electrons and/or protons [2,4–6]. Cooper pairs carry twice the charge of their constituent fermion, while a Bose-Einstein condensate of deuterons carries only once the charge of its (boson) constituent. This system is currently the subject of vigorous experimental pursuit [7].

Mixtures of condensates carrying different electric charges may also apply to ultracold-atomic gases with synthetic gauge field. Recent progress both in theoretical understanding and experimental techniques to control such systems makes it promising that artificial dynamical gauge fields may be realized there [8,9]. In that case, effectively a system could be described by multicomponent charged condensate models. Our present discussion may, in the future, find applications to these systems.

In superconductors with more than two components and $U(1)^N$ broken symmetry there can be pairing transitions to $U(1)^{N-M}$ paired states driven by proliferation of composite vortices [10–12]. Such pairing mechanisms can lead to charge-$4e$ electronic superconducting systems as hypothesized recently in various contexts [1,13,14], along with other recently discussed mechanisms for charge-$4e$ superconductivity [15].

The above examples from superconductivity and superfluidity, along with the multicomponent gauge theories which appear as effective field theories in other condensed matter systems [16,17], calls for investigation of mixtures of charged condensates with arbitrary ratio of condensate charges. To this end we study a phenomenological Ginzburg-Landau model that accounts for such mixtures, regardless of their underlying microscopic origin. We discuss below that if the mixtures of charged condensates carrying different electric charges are realized, either in natural or artificial systems, their response to external applied magnetic field or rotation would be very different from those of mixtures with equal charges. This is because of the substantial difference in the topological excitations as compared to systems where condensates carry the same electric charge.

In Sec. II we introduce a mean-field model that accounts for mixtures of charged condensates, when the condensates carry different electric charges. Section III is devoted to elementary topological excitations, that is fractional vortices, and flux quantization in our Ginzburg-Landau model. In Sec. IV, we investigate the physics of flux carrying topological excitations within the London limit where condensates are assumed to have constant densities.

II. MIXTURES OF CHARGED CONDENSATES

A charged condensate can, under certain conditions, be described by mean-field Ginzburg-Landau free energy that couples it to the vector potential of the magnetic field through the kinetic term

$$\frac{1}{8\pi}|\nabla\times\mathbf{A}|^2+\frac{\hbar^2}{2m}\left|\left(\nabla+i\frac{e^*}{\hbar c}\mathbf{A}\right)\psi\right|^2+V(\psi). \qquad (1)$$

Here e^* is the electric charge of the condensate and m its rest mass. $\hbar$ and c are respectively the reduced Planck constant and the speed of light in the vacuum. V is the interacting potential. For example, for an ordinary superconductor, a Cooper pair has a charge twice that of an electron. Thus, there $e^*=2e$. On the other hand, a Bose-Einstein condensate of singly charged bosons will have electric charge $e^*=e$. Thus mixtures of charged condensates should generically have different couplings to the vector potential. A mixture of condensates with different masses and charges is thus

*garaud.phys@gmail.com

described by

$$\frac{1}{8\pi}|\nabla\times\mathbf{A}|^2+\sum_a\frac{\hbar^2}{2m_a}\left|\left(\nabla+i\frac{e_a}{\hbar c}\mathbf{A}\right)\psi_a\right|^2+V(\psi_a). \quad (2)$$

Note that since the theory is invariant under complex conjugation, it is sufficient to consider positive charge only, without losing generality, condensates with negative charge being obtained by complex conjugation of the one with the positive charge. Now, to get rid of superfluous parameters, we express the energy in units of $\frac{\hbar^2c^2}{4\pi}$ and rescale the fields as

$$\tilde{\mathbf{A}}=\frac{\mathbf{A}}{\hbar c}\ \text{ and }\ \tilde{\psi}_a=\sqrt{\frac{4\pi}{m_ac^2}}\psi_a. \quad (3)$$

Dropping the $\tilde{}$ symbol further on, a mixture of charged condensates is thus described by the free energy density

$$\mathcal{F}=\frac{1}{2}(\nabla\times\mathbf{A})^2+\sum_{a=1,2}\frac{1}{2}|(\nabla+ie_a\mathbf{A})\psi_a|^2+V(\psi_a). \quad (4)$$

Here $\psi_a=|\psi_a|e^{i\varphi_a}$ are complex fields that stand for the charged condensates (with different indices $a=1,2$). The condensates are coupled together through the electromagnetic interactions mediated by the vector potential $\mathbf{A}$ in the kinetic terms $\mathbf{D}\psi_a=(\nabla+ie_a\mathbf{A})\psi_a$. Since ψ_a are condensates that are essentially different, they should be independently conserved. It results that the potential has global $U(1)\times U(1)$invariance ensuring independent conservation of both particle numbers

$$V(\psi_a)=\sum_a\alpha_a|\psi_a|^2+\frac{1}{2}\beta_a|\psi_a|^4. \quad (5)$$

In the condensed phase, α_a are negative parameters while $\beta_a>0$. The model exhibits gauge invariance under local $U(1)$ transformations. That is, for arbitrary $\chi(\mathbf{x})$, the energy (4) is unchanged under the transformations

$$\mathbf{A}\to\mathbf{A}-\nabla\chi,\ \ \psi_a\to e^{ie_a\chi}\psi_a. \quad (6)$$

As will be explained later on, a necessary condition for finite energy flux carrying configurations is that the charge of the condensates should be commensurate. That is, the ratio of the coupling constants e_a is a rational number: $e_1/e_2\in\mathbb{Q}$. To capture this constraint, it is convenient to parametrize the gauge couplings as $e_a=eg_a$, where g_a are integer numbers ($g_a\in\mathbb{Z}$). Moreover, the two integers g_1 and g_2 should be relatively prime (their greatest common divisor must be 1). Within our parametrization, e is an arbitrary number that uniquely parametrizes the London penetration length defined below. If we apply this model to liquid metallic deuterium, the couplings are $(g_1,g_2)=(1,2)$ and ψ_1 denotes the deuteron condensate while ψ_2 (carrying twice the electric charge of ψ_1) denotes electronic Cooper pairs.

Functional variation of the free energy (4) determines the Euler-Lagrange equations of motion. That is, variation with respect to complex fields ψ_a^* gives the Ginzburg-Landau equation for the charged condensates, while variation with respect to the vector potential defines Ampère's law

$$\mathbf{DD}\psi_a=2\frac{\partial V(\Psi)}{\partial\psi_a^*}\quad\text{and}\quad\nabla\times\nabla\times\mathbf{B}=\mathbf{J}, \quad (7)$$

with the supercurrent

$$\mathbf{J}\equiv\sum_a\mathbf{J}^{(a)}=\sum_a e_a\mathrm{Im}(\psi_a^*\mathbf{D}\psi_a). \quad (8)$$

In the ground state, the condensates have constant densities $|\psi_a|=\sqrt{-\alpha_a/\beta_a}$ and $\mathbf{A}$ is a pure gauge. The length scales at which the condensates recover their ground-state value after infinitesimal perturbations, the coherence lengths, are $\xi_a=1/\sqrt{-2\alpha_a}$. The penetration depth of the magnetic field $\lambda=1/e\sqrt{\sum_a g_a^2|\psi_a|^2}$ is consistently derived in Sec. IV.

When considering vortex matter, we restrict ourselves to field configurations varying in the xy plane only and with normal magnetic field, that is, field configurations describing both two-dimensional systems and three-dimensional system invariant under translations along the normal direction. To investigate the physical properties of topological excitations in our model for mixtures of charged condensates, we numerically minimize the free energy (4) within a finite-element framework provided by the FREEFEM++ library [18]. For technical details, see the discussion in Appendix B.

III. TOPOLOGICAL DEFECTS

Because we consider several condensates, the elementary topological excitations are fractional vortices, that is, field configurations with 2π phase winding of a single condensate (e.g., φ_1 has $\oint\nabla\varphi_1=2\pi$ winding while $\oint\nabla\varphi_2=0$). A fractional vortex carries a fraction of the flux quantum. This can be seen by deriving the quantization condition for the magnetic flux. The supercurrent (8), defined from Ampère's equation $\nabla\times\mathbf{B}+\mathbf{J}=0$, reads as

$$\mathbf{J}:=\frac{\delta\mathcal{F}}{\delta\mathbf{A}}=e^2\varrho^2\mathbf{A}+e\sum_a g_a|\psi_a|^2\nabla\varphi_a. \quad (9)$$

Here we defined the *weighted* density $\varrho^2=\sum_a g_a^2|\psi_a|^2$. Since the supercurrent $\mathbf{J}$ is screened, it decays exponentially and the magnetic flux thus reads as

$$\begin{aligned}\Phi&=\int\mathbf{B}\cdot d\boldsymbol{S}=\oint\mathbf{A}\cdot d\boldsymbol{\ell}\\&=\frac{1}{e^2\varrho^2}\oint\left(J-e\sum_a g_a|\psi_a|^2\nabla\varphi_a\right)\cdot d\boldsymbol{\ell}\\&=-\frac{1}{e\sum_b g_b^2|\psi_b|^2}\sum_a g_a|\psi_a|^2\oint\nabla\varphi_a\cdot d\boldsymbol{\ell}. \quad (10)\end{aligned}$$

Since the condensates ψ_a are complex fields, their phases wind integer number of time. The couple (k_1,k_2) denotes the field configurations with winding k_a of the condensate ψ_a. The elementary excitations are fractional vortices (1,0) and (0,1) with unit winding in each component. A given fractional vortex in the condensate a thus carries a fraction of the magnetic flux $\Phi_a/\Phi_0=g_a|\psi_a|^2/\varrho^2$. Here $\Phi_0=2\pi/e$ is the flux quantum. For the magnetic flux to be quantized, as long as $g_1\neq g_2$, it is necessary that different condensates have different winding number k_a. This follows from

$$\sum_a g_a\frac{\Phi_a}{\Phi_0}=\frac{\sum_a g_a^2|\psi_a|^2}{\sum_b g_b^2|\psi_b|^2}=1. \quad (11)$$

When both condensates carry the same electric charge, $g_1 = g_2 = 1$, the quantization condition (11) reduces to the quantization conditions for multiband/multicomponent superconductors [19].

Thus, each condensate a has to wind $k_a = g_a$ times, so that the resulting composite vortex carries one flux quantum $\Phi_0 = 2\pi/e$. Fractional vortices have logarithmically divergent energy per unit length and thus cannot form in bulk systems [19]. This can be seen by rewriting the free energy into *charged* and *neutral* modes. For this, and using (9), the kinetic term can be rewritten

$$\frac{1}{2}\sum_a |\mathbf{D}\psi_a|^2 = \frac{1}{2}\sum_a \{(\boldsymbol{\nabla}|\psi_a|)^2 + |\psi_a|^2(\boldsymbol{\nabla}|\varphi_a|)^2\} + \frac{\mathbf{J}^2}{2e^2\varrho^2} - \frac{\left(\sum_a g_a|\psi_a|^2\boldsymbol{\nabla}\varphi_a\right)^2}{2\varrho^2}, \tag{12}$$

with again the *weighted* density $\varrho^2 = \sum_a g_a^2|\psi_a|^2$. Defining the *weighted* phase difference $\varphi_{12} \equiv g_1\varphi_2 - g_2\varphi_1$, the free energy (4) reads as

$$\mathcal{F} = \frac{1}{2}(\boldsymbol{\nabla}\times\mathbf{A})^2 + \frac{\mathbf{J}^2}{2e^2\varrho^2} \tag{13a}$$

$$+ \sum_a \frac{1}{2}(\boldsymbol{\nabla}|\psi_a|)^2 + \alpha_a|\psi_a|^2 + \frac{\beta_a}{2}|\psi_a|^4 \tag{13b}$$

$$+ \frac{|\psi_1|^2|\psi_2|^2}{2\varrho^2}(\boldsymbol{\nabla}\varphi_{12})^2. \tag{13c}$$

Since it decouples from the gauge field, the term (13c) is called *neutral mode*. This is the kinetic energy of the relative motion of the two condensates. That is, the codirected (counterdirected) motion of particles with opposite (alike) charges e_a. When φ_{12} has a winding, this neutral mode has logarithmically divergent energy. Indeed, asymptotically each phase is well approximated by $\varphi_a = k_a\theta$, where k_a are the (integer) vorticities and θ the polar angle. The condition for

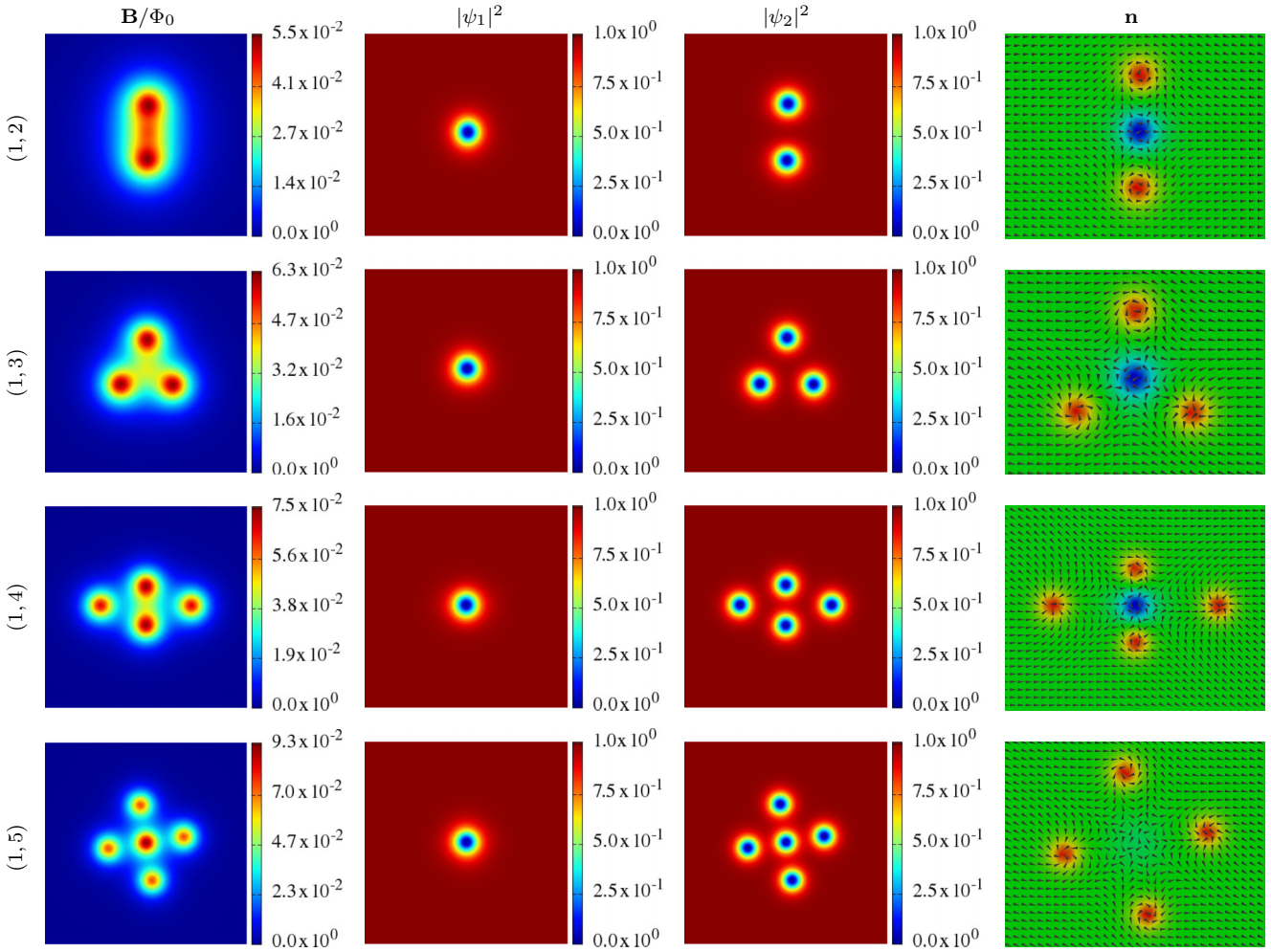

FIG. 1. (Color online) Molecule-like topological excitations carrying a unit flux quantum. The parameters of the Ginzburg-Landau functional (4) are $(\alpha_a,\beta_a) = (-3,1)$, for both condensates ($a = 1,2$) and $e = 0.2$. Each row displays solutions for different winding parameters (g_1,g_2) (indicated on left). Displayed quantities in each row are respectively the magnetic field $\mathbf{B}$ (divided by the flux quantum Φ_0) and the densities of both condensates $|\psi_1|^2$ and $|\psi_2|^2$ (in units of their ground-state value). The rightmost panel shows the normalized projection of the pseudospin $\mathbf{n}$ (15) onto the plane, while the color scheme indicates the magnitude of n_z. Blue corresponds to the south pole (-1) while red is the north pole $(+1)$ of the target sphere S^2.

the logarithmic divergence to be absent and thus for the energy to be finite thus reads as

$$0 = \oint \nabla\varphi_{12} \cdot d\boldsymbol{\ell} = \oint \nabla(g_1\varphi_2 - g_2\varphi_1) \cdot d\boldsymbol{\ell} = (g_1k_2 - g_2k_1). \quad (14)$$

For a configuration carrying a single flux quantum (and since g_a and k_a are integers), the absence of winding in the weighted phase difference dictates that $k_a = g_a$. Thus the configurations which have no logarithmic divergence winds g_1 times in ψ_1 and g_2 times in ψ_2. Note that this condition also implies that the total flux is integer (11). On the other hand, fractional vortices have logarithmically divergent energy. This is because they have winding in the *weighted* phase difference. That is, when $g_2k_1 \neq g_1k_2$, since the screening is incomplete, the energy of the vortex grows with the system size. Such vortices are typically thermodynamically unstable in bulk systems. When both condensates carry the same electric charge $g_1 = g_2 = 1$, the condition (14) is automatically satisfied, provided both condensates have the same winding $k_1 = k_2$. That is, only co-centered composite vortices with same winding in both condensates have finite energy. Since fractional vortices have logarithmically divergent energy per unit length, they cannot form in bulk systems [20].

Consider now the simplest case where the condensate ψ_1 carries single charge while ψ_2 carries double: $(g_1,g_2) = (1,2)$. The resulting composite vortex carrying one flux quantum is the bound state of one (fractional) vortex in ψ_1 and two vortices in ψ_2. To reduce the cost of kinetic energy in the neutral sector, the interaction through the neutral sector binds vortices together. It is minimal when cores in different condensates coincide (see discussion below in Sec. IV). However the two vortices in ψ_2 quite naturally repel each other, as would two Abrikosov vortices do in single-band systems. As a result we can expect that if the magnetic repulsion is strong enough, despite the attractive channel through the neutral sector, fractional vortices will not overlap. This is indeed the case, as shown in Fig. 1. The regime shown on the first line has $(g_1,g_2) = (1,2)$, so the condensates have single and double winding, respectively. The resulting topological defect, carrying a single flux quantum, is a bound state of fractional vortices that are not co-centred and the configuration looks like an elongated rod. We refer to such bound state as a vortex molecule [21].

Bound states of nonoverlapping fractional vortices feature special topological properties that motivate their denomination as skyrmions. The terminology follows from the fact that two-component models can be mapped to easy-plane nonlinear σ models that are associated with a $\mathbb{C}P^1$ topological invariant [22–24]. In systems with the same charge of both condensates, the two-component model is rewritten in term of the total current $\mathbf{J}$, the total density $\tilde{\varrho}^2 = \sum_a |\psi_a|^2$, and the pseudospin $\mathbf{n}$. The pseudospin unit vector is the projection of the superconducting condensates on spin-1/2 Pauli matrices $\boldsymbol{\sigma}$:

$$\mathbf{n} \equiv (n_x,n_y,n_z) = \frac{\Psi^\dagger \boldsymbol{\sigma} \Psi}{\Psi^\dagger \Psi}. \quad (15)$$

When all condensates have the same couplings g_a, the spinor Ψ is defined as the two-vector of complex condensates $\Psi^\dagger = (\psi_1^*,\psi_2^*)$. The finiteness of the energy dictates that $\mathbf{n}$ is asymptotically a constant vector, while vanishing of neutral modes implies that $n_x + in_y \propto e^{i(\varphi_2-\varphi_1)}$ has no winding.

To obtain a similar projection for incommensurate charges, the spinor Ψ should be chosen so that the pseudospin does not wind asymptotically (when neutral mode vanish). There are several possibilities to realize such a projection and we choose

$$\Psi^\dagger = (|\psi_1|e^{-ig_2\varphi_1},|\psi_2|e^{-ig_1\varphi_2}). \quad (16)$$

The projection (15) of (16) maps to the two-sphere target space. It determines the pseudospin $\mathbf{n}$ that we use along the paper for the visualization of the pseudospin texture. Note that (16) is a nonholomorphic map, so it hard to justify the quantization of the associated invariant. For this we introduce another map which is holomorphic:

$$\Psi^\dagger = \left(\psi_1^{*g_2},\psi_2^{*g_1}\right). \quad (17)$$

The associated projection is a map from the one-point compactification of the plane ($\mathbb{R}^2 \cup \{\infty\} \simeq S^2$) to the two-sphere target space spanned by $\mathbf{n}$. That is $\mathbf{n} : S^2 \to S^2$, which is classified by the homotopy class $\pi_2(S^2) \in \mathbb{Z}$. This defines the integer-valued $\mathbb{C}P^1$ topological charge

$$\mathcal{Q}(\mathbf{n}) = \frac{1}{4\pi}\int_{\mathbb{R}^2} \mathbf{n} \cdot \partial_x\mathbf{n} \times \partial_y\mathbf{n}\, dxdy = g_1g_2. \quad (18)$$

If $\Psi \neq 0$ everywhere, $\mathcal{Q}$ is an integer number. Roughly speaking, $\mathcal{Q}$ counts the number of times the texture $\mathbf{n}$ (15) covers the target S^2 sphere. For practical purposes, and since it gives much better accuracy, we compute the degree of the maps (16) or (17), instead of computing the formula (18). Numerically calculated topological charge for the various configurations we constructed is indeed found to be integer (with a negligible error of order 10^{-4}).

The map (17) provides a rigorous justification of the topological invariant (18), but the associated texture $\mathbf{n}$ turns out to be very difficult to visualize. So we still use (16) that gives more straightforward physical interpretation for the visualization of the pseudospin texture. Interestingly, when computed numerically both definitions give similar result and accuracy of the topological charge.

In our parametrization of the gauge couplings $e_a = eg_a$, the charges of the condensates are commensurate. That is, their ratio is a rational number and the simplest case we discussed is $(g_1,g_2) = (1,2)$. There, the unit flux quantum excitation is a molecule made of two fractional vortices in ψ_2 bound together by a single vortex in the ψ_1 condensate. For different ratio of the gauge couplings, the unit flux molecule-like bound states assume very rich structures as shown in Fig. 1 for $g_1 = 1$ and $g_2 = 2,3,4,5$. There, depending on the vorticities, fractional vortices can either be completely split apart or partially overlapping, as for example in $(g_1,g_2) = (1,5)$. The topological properties when fractional vortices overlap are essentially different than when they do not. Indeed the topological charge (18) is quantized only if there is no core overlap. To emphasize the richness in unit flux structures, we display in Fig. 2 configurations with other ratios of the commensurate charges. All of these have nontrivial, very different signature of the magnetic field. The structure of the molecule-like bound state depends not only on the ratio of the gauge couplings but also on the ratio $m = |\psi_1|^2/|\psi_2|^2$ of

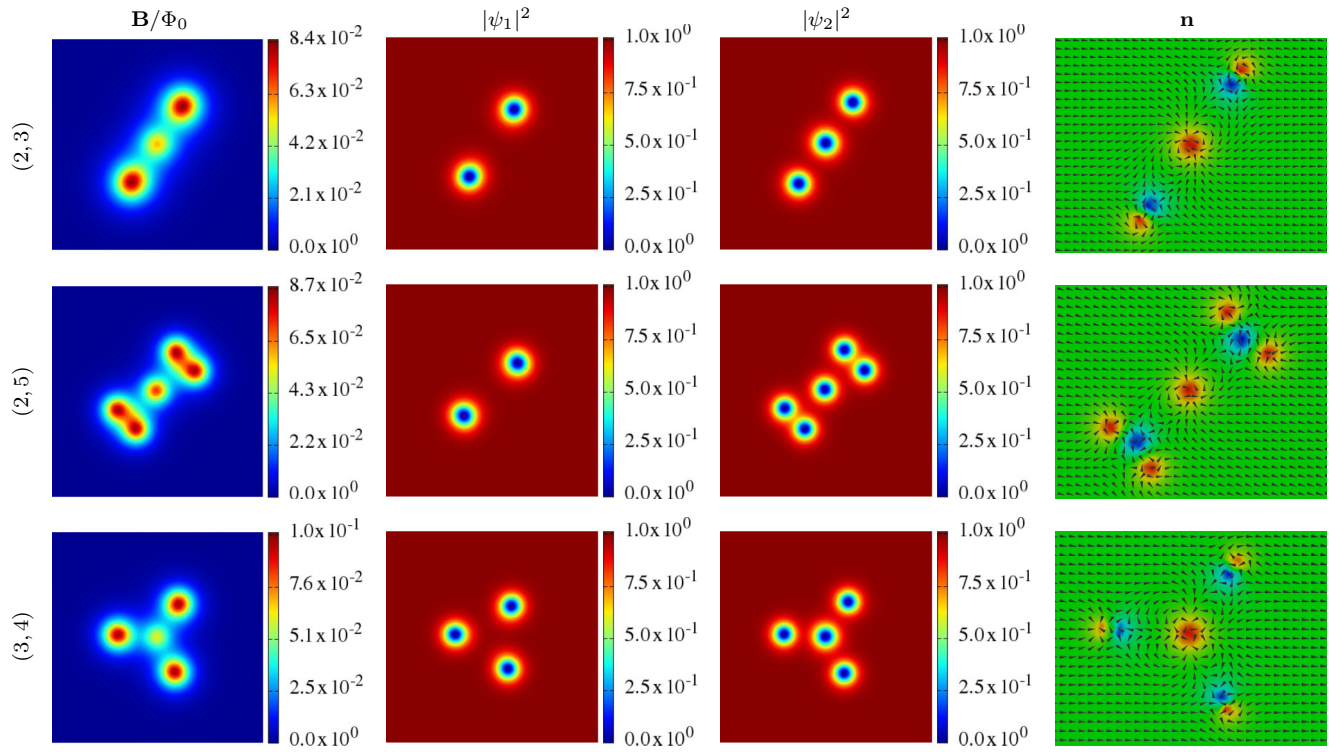

FIG. 2. (Color online) Molecule-like configurations of topological excitation carrying a unit flux quantum, for various values of winding parameters (g_1, g_2) (indicated on the left). The parameters of the Ginzburg-Landau functional and the displayed quantities are the same as in Fig. 1.

the densities associated with each condensate. This can be seen from additional regimes we displayed in Appendix A.

As discussed later on in Sec. IV, depending on the ratio of densities in both condensates, the structure of the single flux quantum topological defect can be quite different. Indeed for substantial disparity in densities the "symmetric molecule" structure, dominated by the long-range quadrupolar mode of the relative phase φ_{12}, is no longer preferred. Instead, an "asymmetric molecule" is formed and it is characterized by a longer range dipolar mode of the relative phases. Such regimes with disparity in the condensate densities can be seen in Fig. 3. More regimes are given as additional material in Appendix A.

A. A closer look at liquid metallic deuterium–like system

We argued that our model captures topological aspects of mixtures of condensates with commensurate charges and that it qualitatively applies to various systems and for example to the superconducting state for liquid metallic deuterium (LMD), where one expects coexistence of electronic Cooper pairs and Bose condensate of deuterons. Since reliable microscopic parameters for this state are not available we will study a phenomenological Ginzburg-Landau model for such a mixture of charged condensates. The deuterium nucleus (deuteron) is a spin-1 particle that can condense in several states [4,5]. Here we ignore spin degrees of freedom and treat it as a scalar charged condensate carrying electric charge $+e$, while electronic Cooper pairs carry charge $-2e$. The mass of the electronic Cooper pairs is $m = 2m_e \approx 1$ MeV$/c$ while the mass of the deuteron is $m_d \approx 1875$ MeV$/c$. Let ψ_1 and ψ_2 respectively denote the deuteronic and electronic condensates, so $(g_1, g_2) = (1,2)$. Because of the electric neutrality at zero temperature we consider

$$m_1|\tilde{\psi}_1|^2 = 2m_2|\tilde{\psi}_2|^2, \tag{19}$$

[note for this expression we restore the ˜ symbols from (3)]. Thus in this regime the electronic condensate is responsible for 99.9% of the screening of the flux. In Fig. 3, we show a single flux quantum topological defect for big disparity in ground-state densities that are likely to occur for liquid metallic deuterium. There, the arrangement of fractional vortices is somewhat different from those displayed in Fig. 1. Indeed, unlike previously, some of the fractional vortices overlap. The relative phase φ_{12} corresponding to the regime Fig. 1 assumes quadrupolar structure. The relative phases corresponding to Fig. 3 instead show a dipolar structure. This is shown in Fig. 4. Dipole modes are longer range than quadrupole modes. This change in the long-range behavior of the relative phases should result in important modification of the large-scale vortex matter structures. Long-range dipolar modes were shown to play an important role, although in a different context, on large-scale vortex structure formation [24]. As discussed below in Sec. IV, the modification of the long-range modes is consistently reproduced in the London approximation.

Here two constituent fractional vortices overlap. As a result, the topological invariant (18) here is not quantized. This can be heuristically understood by the fact that the target sphere is not completely covered. With our crude estimates the ratio of condensate densities for liquid metallic deuterium is about the same as for liquid metallic hydrogen. However because the commensurate charges are different, the

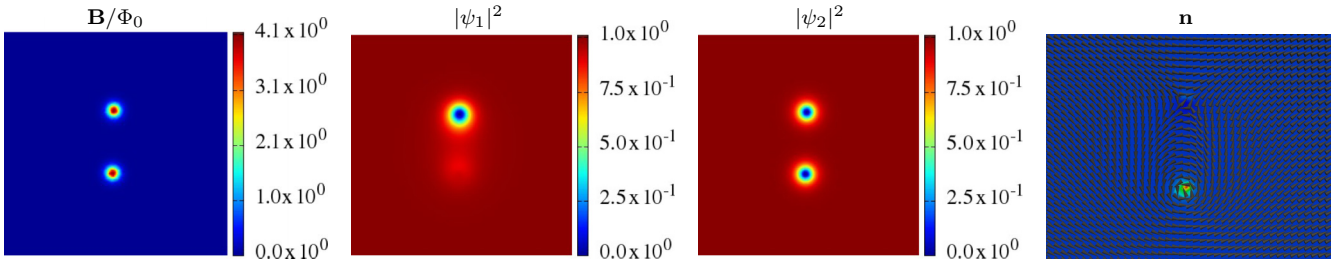

FIG. 3. (Color online) Vortex solutions carrying a single flux quantum for parameters of the Ginzburg-Landau functional (4) giving a big disparity in condensate densities. The winding parameters here are $(g_1,g_2)=(1,2)$. The other parameters are $(\alpha_1,\beta_1)=(-10,10)$, $(\alpha_2,\beta_2)=(-10,0.01)$, and $e=0.2$. This choice follows crude estimation (19) of relative condensate densities in the case of the superconducting state of liquid metallic deuterium. Displayed quantities are the same as in Fig. 1. Note here that the pseudospin texture $\mathbf{n}$ is mostly located *almost* to the south pole of the target sphere because of the very big disparity in densities. That is, since $|\psi_1|^2 \ll |\psi_2|^2$, then $n_z=\frac{|\psi_1|^2-|\psi_2|^2}{|\psi_1|^2+|\psi_2|^2}\approx -1$ everywhere except at the core of ψ_2 that does not overlap with the core in ψ_1. Note that since the core in ψ_1 coincides with a core in ψ_2, the south pole $n_z=-1$ is never reached.

topological excitations are completely different. The lowest energy topological excitation in a liquid metallic hydrogen–like system is an axially symmetric composite vortex, while for LMD it is a composite object of two co-centered vortices plus one satellite fractional vortex. The magnetic signature of the topological defect in LMD looks like a pair of vortices, while it is a single vortex for LMH.

B. The case of incommensurate charges

The conditions for finite-energy solutions (14) and the flux quantization (11) rely on the fact that charges are commensurate, that is, that their ratio is a rational number so that they can be parametrized as $e_a=eg_a$, where g_a are integer numbers. For generality, here we address the question of what changes if charged condensates have incommensurate electric charges. When e_a stands for elementary charges of elementary particles, they are integer multiples of an elementary electric charge. With current progress in creation of artificial gauge fields it cannot be ruled out that systems with incommensurate coupling to the gauge field may be artificially realized.

For this exercise, we have to relax the condition that g_a are both integer numbers. Since k_a have to be integer for the ψ_a's to be single valued, the condition (14) ensuring both finite energy and flux quantization cannot be satisfied. As a result, the elementary vortices carry different flux Φ_a that cannot be added together to add up to a flux quantum. More precisely,

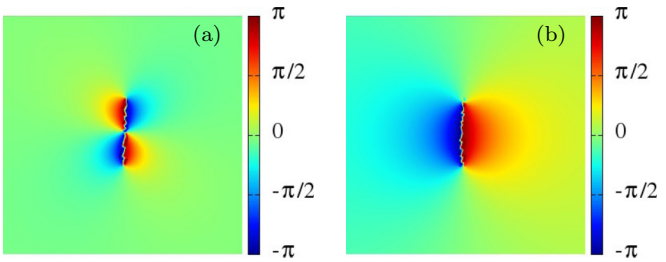

FIG. 4. (Color online) This shows the relative phases $\varphi_{12}=g_1\varphi_2-g_2\varphi_1$, for single flux quantum topological defect with vorticities $(g_1,g_2)=(1,2)$. The left panel (a) with quadrupole structure corresponds to the regime in Fig. 1. On the other hand, the right panel (b) corresponding to Fig. 3 has dipole structure which is longer range.

the total flux (10) is

$$\Phi = k_1\frac{2\pi g_1|\psi_1|^2/e}{g_1^2|\psi_1|^2+g_2^2|\psi_2|^2}+k_2\frac{2\pi g_2|\psi_2|^2/e}{g_1^2|\psi_1|^2+g_2^2|\psi_2|^2} = k_1\Phi_1+k_2\Phi_2, \tag{20}$$

and it is impossible to (consistently) write this as an integer times a flux quantum Φ_0. Correspondingly, when charges are incommensurate, it is not possible by any means to eliminate the winding in the neutral sector (13c). Thus there are no finite-energy solutions (in infinite domain). Instead solutions have logarithmically divergent energy due to the (superfluid) mode associated with the neutral sector. That is, a phase gradient resulting from a phase winding always causes logarithmic divergence of vortex energy and cannot be fully compensated by the vector potential.

Let us now close this remark about mixtures of condensates with incommensurate charges, and focus on the case where the ratio of the coupling constants e_a is a rational number. That is $e_a=eg_a$ where g_a are integers. We found that topological defects carrying integer flux are bound states of different fractional number of vortices in the different condensates. Because of the frustrated interactions that vortices in the same condensate repel, while they try to overlap with vortices in the other condensate, these bound states arrange into very complicated molecule-like structures. A large part of this exotic vortex structures can be captured by investigating the London limit, where fractional vortices can be mapped to Coulomb charges.

IV. LONDON LIMIT

When the electromagnetic repulsion is strong enough, integer vortices split to form a bound state of fractional vortices. The underlying physics describing the core splitting can be accurately captured within the London approximation where $|\psi_a|=\text{const}$ everywhere (except for a sharp cutoff at vortex core). There, the expression (13) further simplifies to

$$\mathcal{F}=\frac{1}{2}\left(\mathbf{B}^2+\frac{1}{e^2\varrho^2}|\nabla\times\mathbf{B}|^2\right) \tag{21a}$$

$$+\frac{|\psi_1|^2|\psi_2|^2}{2\varrho^2}(\nabla\varphi_{12})^2. \tag{21b}$$

The interaction energy of two nonoverlapping fractional vortices is approximated in this London limit by considering *charged* (21a) and *neutral* modes (21b), separately. The energy of the *charged* sector (21a) reads as

$$F_{\rm mag} = \int \frac{\mathbf{B}}{2}(\mathbf{B} + \lambda^2 \nabla \times \nabla \times \mathbf{B}), \tag{22}$$

where the London penetration length is $\lambda = 1/e\varrho$. The London equation for a (point-like) vortex placed at $\mathbf{x}_a$ and carrying a flux Φ_a is

$$\lambda^2 \nabla \times \nabla \times \mathbf{B} + \mathbf{B} = \Phi_a \delta(\mathbf{x} - \mathbf{x}_a), \tag{23}$$

and its solution is

$$\mathbf{B}_a(\mathbf{x}) = \frac{\Phi_a}{2\pi\lambda^2} K_0\left(\frac{|\mathbf{x} - \mathbf{x}_a|}{\lambda}\right), \tag{24}$$

where K_0 is the modified Bessel function of the second kind. For two vortices located at $\mathbf{x}_a$ and $\mathbf{x}_b$, respectively carrying fluxes Φ_a and Φ_b, the source term in the London equation reads as $\Phi_a\delta(\mathbf{x} - \mathbf{x}_a) + \Phi_b\delta(\mathbf{x} - \mathbf{x}_b)$ and the magnetic field is the superposition of two contributions $\mathbf{B}(\mathbf{x}) = \mathbf{B}_a(\mathbf{x}) + \mathbf{B}_b(\mathbf{x})$. Thus

$$\begin{aligned} F_{\rm mag} &= \int \frac{1}{2}(\mathbf{B}_a + \mathbf{B}_b)[\Phi_a\delta(\mathbf{x} - \mathbf{x}_a) + \Phi_b\delta(\mathbf{x} - \mathbf{x}_b)] \\ &= \frac{\Phi_a\Phi_b}{2\pi\lambda^2} K_0\left(\frac{|\mathbf{x}_2 - \mathbf{x}_1|}{\lambda}\right) + E_{va} + E_{vb}, \end{aligned} \tag{25}$$

and $E_{va} \equiv \int \mathbf{B}_a(\mathbf{x}_a)\Phi_a/2$ is the (self-)energy of the vortex a. Finally, the interaction energy of two vortices in components a,b reads as

$$E_{ab}^{\rm (int),mag} = \frac{2\pi g_a g_b |\psi_a|^2|\psi_b|^2}{\varrho^2} K_0\left(\frac{|\mathbf{x}_a - \mathbf{x}_b|}{\lambda}\right). \tag{26}$$

The interaction through the charged sector is thus screened interaction given by the modified Bessel function. When the couplings e_a are parametrized such that they have the same sign (since the theory is invariant under complex conjugation, this is always possible), this interaction is always positive for any a,b having the same sign of vorticity. It then gives repulsive interaction between any kind of fractional vortices with codirected winding. That is, vortices repel while a vortex and an antivortex attract each other. On the other hand, the interaction through the *neutral* sector is attractive (resp. repulsive) for fractional vortices of the different (resp. same) condensate. The energy associated with the *neutral* mode (21b) reads as

$$F_{\rm neutral} = \frac{|\psi_1|^2|\psi_2|^2}{2\varrho^2} \int (\nabla\varphi_{12})^2. \tag{27}$$

To evaluate the interaction between fractional vortices in different condensates and respectively located at $\mathbf{x}_1$ and $\mathbf{x}_2$, the neutral sector is expanded:

$$\begin{aligned} F_{\rm neutral} =& \frac{|\psi_1|^2|\psi_2|^2}{2\varrho^2} \int (g_2\nabla\varphi_1)^2 + (g_1\nabla\varphi_2)^2 \\ &- 2g_1g_2\nabla\varphi_1 \cdot \nabla\varphi_2. \end{aligned} \tag{28}$$

At sufficiently large distance, a phase winding around some singularity located at a point $\mathbf{x}_a$ is well approximated by $\varphi_a = \theta$. Thus

$$\nabla\varphi_a = \frac{\mathbf{e}_\theta}{|\mathbf{x} - \mathbf{x}_a|} = z \times \nabla \ln|\mathbf{x} - \mathbf{x}_a|. \tag{29}$$

As a result, the interaction part in the neutral sector reads as

$$\begin{aligned} E_{12}^{\rm (int),neutral} &= -\frac{g_1g_2|\psi_1|^2|\psi_2|^2}{\varrho^2} \int \nabla\varphi_1 \cdot \nabla\varphi_2 \\ &= 2\pi g_1 g_2 \frac{|\psi_1|^2|\psi_2|^2}{\varrho^2} \ln|\mathbf{x}_2 - \mathbf{x}_1|. \end{aligned} \tag{30}$$

Similarly, the interaction between two vortices in the same condensate a is computed by requiring that the phase be the sum of the individual phases $\varphi_a = \varphi_a^{(1)} + \varphi_a^{(2)}$, while $\varphi_b = 0$. Then the interaction reads as

$$E_{aa}^{\rm (int),neutral} = -2\pi g_b^2 \frac{|\psi_1|^2|\psi_2|^2}{\varrho^2} \ln\left|\mathbf{x}_a^{(2)} - \mathbf{x}_a^{(1)}\right|, \tag{31}$$

with here $b \neq a$. To summarize, the interaction of vortices in different condensates is

$$\frac{E_{12}^{\rm (int)}}{2\pi} = g_1g_2 \frac{|\psi_1|^2|\psi_2|^2}{\varrho^2}\left[\ln\frac{r}{R} + wK_0\left(\frac{r}{\lambda}\right)\right], \tag{32}$$

while interactions of vortices of similar condensates are

$$\frac{E_{aa}^{\rm (int)}}{2\pi} = -\frac{g_b^2|\psi_1|^2|\psi_2|^2}{\varrho^2} \ln\frac{r}{R} + \frac{g_a^2|\psi_a|^4}{\varrho^2} K_0\left(\frac{r}{\lambda}\right), \tag{33}$$

with $b \neq a$, $r \equiv |\mathbf{x}_a - \mathbf{x}_b|$, and R the sample size. Choosing the energy scale to be $2\pi g_1g_2|\psi_1|^2|\psi_2|^2/\varrho^2$ and defining the parameters

$$s = \frac{g_1}{g_2} \quad \text{and} \quad m = \frac{|\psi_1|^2}{|\psi_2|^2}, \tag{34}$$

the interaction between fractional vortices reads as

$$\begin{aligned} E_{11}(r) &= \frac{1}{s}\ln\frac{R}{r} + \frac{m}{s}K_0\left(\frac{r}{\lambda}\right), \\ E_{22}(r) &= s\ln\frac{R}{r} + \frac{s}{m}K_0\left(\frac{r}{\lambda}\right), \\ E_{12}(r) &= -\ln\frac{R}{r} + K_0\left(\frac{r}{\lambda}\right). \end{aligned} \tag{35}$$

Thus vortex matter in the London limit of a two-component superconductor with incommensurate charges is described by a 3-parameter family (m,s,R). This is illustrated in Fig. 5.

The interaction between vortices in the same condensates is repulsive. In multicomponent superconductors where both condensates have the same number of vortices in each component, vortices in different condensates will attract each other to form a bound state of co-centered vortices that minimizes the energy cost of the neutral sector [19,25]. The situation here is more subtle. Because both condensates have different number of (fractional) vortices, the system has to compromise between vortices in similar condensates that repel each other and the fact that vortices in different condensates try to overlap. This explains why, beyond the London limit (see, e.g., Fig. 1), integer vortices form a molecule-like bound state of split fractional vortices.

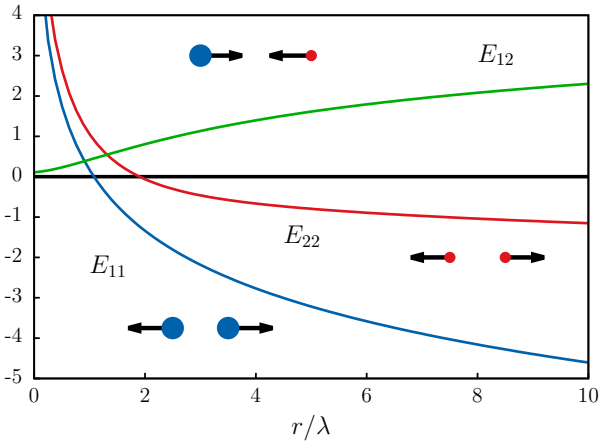

FIG. 5. (Color online) Interaction energies between pointlike charges associated with vortices in different condensates. The blue (big) dot represents the vortex in ψ_1 while the red (small) dots represent the vortices in ψ_2. Here we chose $m = 0.2$ and $s = 1/2$. Alike charges always repel while different charges attract with long-range logarithmic attraction.

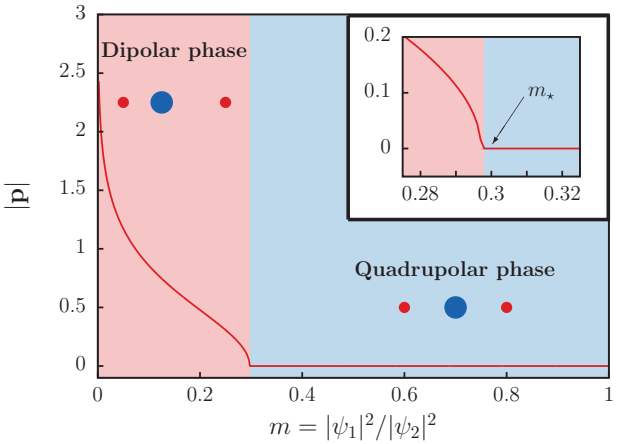

FIG. 6. (Color online) Structure of the single skyrmion for $g_1 = 1$ and $g_2 = 2$ as a function of relative ground-state densities of the two condensates. There is a transition in the dipole moment of the molecule. The inset shows that transition closely. When ground-state densities are quite similar, the molecule is symmetric, and it has zero dipole moment. Below a certain threshold $m_\star$, the molecule becomes asymmetric and it develops a nonzero dipole moment. The blue (big) dot represents the vortex in ψ_1 while the red (small) dots represent the vortices in ψ_2.

A. Transition in the structure of the skyrmion

In the context of the mapping to point charges, the finite-energy condition (14) is equivalent to requiring charge neutrality. Thus we complete the mapping to point charges by defining the electric charge $q_2 = g_1$ and $q_1 = -g_2$. A neutral set of charged particle thus satisfy the charge neutrality

$$\sum_a q_a k_a = 0. \tag{36}$$

We already know, from our solutions of the full nonlinear model, that vortex solutions do exist and they have both finite energy and carry unit flux quanta. We also observed that, provided e is small enough, that cores of fractional vortices are not superimposed. We now try to reproduce our results, using the Eqs. (35) of the London limit. Here since a vortex configuration is a neutral set of discrete charge, it can be globally described by its dipole p_i and quadrupole moments d_{ij} in two dimensions:

$$\begin{aligned} p_i &= \sum_a q_a r_i^{(a)}, \\ d_{ij} &= \sum_a q_a \left(2 r_i^{(a)} r_j^{(a)} - \delta_{ij} r_i^{(a)\,2}\right). \end{aligned} \tag{37}$$

The minimum of the interaction energy (35) should describe the location of vortex cores. We apply this for a single vortex with $(g_1, g_2) = (1,2)$. Thus it is described by a set of three point particles, two carrying a single positive charge and one twice negatively charged. According to the interaction energies, it forms a bound state of nonoverlapping particles; see Fig. 6. Remarkably there is a transition of the "molecular" structure at a given $m = m_\star \approx 0.29714$. For $m > m_\star$, the molecule is symmetric and it has no dipole moment. The long-range interactions are thus dominated by quadrupole modes. For sufficient disparity in densities, when $m < m_\star$, the least energetic arrangement is no longer symmetric and thus the vortex molecule develops a dipole moment that is long range and should dramatically alter the large-scale structures. Indeed, quadrupole modes are smaller in amplitude and also decay faster than dipole modes. For examples of the effect of long-range dipolar interactions in large-scale structures (in a different context), see [24].

In our estimates to describe liquid metallic deuterium, the London limit parameter $m = |\psi_1|^2/|\psi_2|^2 \ll 1$. Thus according to the London limit picture Fig. 6, the single flux quantum vortex in the superconducting phase of liquid metallic deuterium should sit in the dipolar regime. As we illustrated in Fig. 3, this is indeed the case, and there is perfect agreement between the London limit picture and direct numerical simulations.

Note that since the model describes independently conserved condensates, it has $U(1) \times U(1)$ invariance. Then both condensates have in principle different critical temperatures at which they condense. Then, there is in principle also always a regime where one of the condensates has much less density than the other. So there is always, at least, a regime where $m \ll 1$ (resp. $m \gg 1$) if ψ_1 (resp. ψ_2) condenses first. So there is always a phase dominated by the long-range dipolar mode in the relative phases, that should dramatically influence large-scale structuring of the vortex matter.

B. The case of many particles

The physics of the topological defects carrying a single flux quantum is shown to be quite rich. Indeed even in the simplest case when $(g_1, g_2) = (1,2)$, the single skyrmion has a transition in its internal structure (see Fig. 6). The emerging long-range modes should have a very important influence on the many-skyrmion states. Investigating the many-skyrmion states may give valuable information about the transport properties or about the lattice structures and their melting. Within the London limit, such properties can be investigated

using molecular dynamics or Monte Carlo simulations of the point particles interacting according to (35). Although the point-charge model does not completely capture all the underlying physics, it can reproduce several aspects of the structures obtained beyond the London limit. This is beyond the scope of the current paper, yet we can address few general comments about the case of many particles.

In order to investigate the many-body properties of our model, one approach is to model fractional vortices by point charges with elementary interactions (35), that is, to consider a set of N_a particles corresponding to (fractional) vortices in the condensate a. For a system containing integer flux, the number of particles should satisfy the relation $g_2 N_1 = g_1 N_2$. The interacting energy in the case of many particles reads as

$$E = \sum_{i=1}^{N_1}\sum_{j>i}^{N_1} E_{11}\left(\left|\mathbf{x}_i^{(1)} - \mathbf{x}_j^{(1)}\right|\right) + \sum_{i=1}^{N_2}\sum_{j>i}^{N_2} E_{22}\left(\left|\mathbf{x}_i^{(2)} - \mathbf{x}_j^{(2)}\right|\right) + \sum_{i=1}^{N_1}\sum_{j=1}^{N_2} E_{12}\left(\left|\mathbf{x}_i^{(1)} - \mathbf{x}_j^{(2)}\right|\right), \tag{38}$$

where $\mathbf{x}_i^{(a)}$ denotes the position of the ith vortex of the condensate a and interaction energies E_{ab} are given by (35). Note that this problem is related to the problem of unconventional plasma discussed in the context of quantum Hall states [26–28].

The many-particle problem (38) can be investigated using different standard techniques such as molecular dynamics or Monte Carlo simulations. In the light of the complicated structure of the single skyrmions, one may expect very rich phases of the vortex matter there. However this deserves full investigation that is beyond the scope of the current paper.

V. CONCLUSIONS

We investigated physical properties of mixtures of charged (bosonic) condensates, carrying different electric charges. More precisely, we introduced a Ginzburg-Landau model that accounts phenomenologically for such mixtures. Disregarding the underlying microscopic theories that describe mixtures of charged condensates, this model is expected to qualitatively describe the topological excitations therein.

Elementary topological excitations are fractional vortices, that is, vortex configurations with winding in only one condensate. Because of the existence of a neutral mode, describing relative counterdirected motion of particles, fractional vortices have logarithmically divergent energy. The condition for having a finite-energy solution in a mixture of condensates having commensurate electric charges $e_1 = g_1 e$ and $e_2 = g_2 e$ is that the phase should wind g_1 times in ψ_1 and g_2 times in ψ_2. Because of the commensuration of electric charge, finite-energy configurations have different number of fractional vortices in different condensates.

Fractional vortices in the same condensate repel while fractional vortices in different condensates attract each other in order to reduce the energy cost associated with the counterflow of charge carriers. As a compromise, the topological excitation carrying an integer flux quantum can form a molecule-like bound state of fractional vortices, where there is no overlapping of vortices in contrast to systems with the same charges [19,24].

We also addressed the question of the underlying topology. There, we showed that two configurations carrying an integer flux quantum are differentiated from each other by a $\mathbb{C}P^1$ topological invariant. The topological excitations were explicitly constructed numerically and their structure, namely the spatial arrangement of constituent fractional vortices, can be understood by investigating the London limit physics, where fractional vortices are mapped to point Coulomb charges.

The model we introduced and its topological excitations applies, at least qualitatively, to various physical systems where different condensates are formed and where they are commensurately coupled to the vector potential of the magnetic field. Namely it could effectively describe the projected superconducting state of liquid metallic deuterium where deuterons form a charged Bose-Einstein condensate mixed with electronic Cooper pairs. This state of matter is currently a subject of experimental pursuit [7]. Since these experiments are conducted in diamond anvil cell that can be equipped with a receiving coil, the finding which we report could help to confirm or rule out formation of this state. Mixtures of commensurately charged condensates might also be an interesting system to be realized in cold atoms with synthetic gauge fields.

ACKNOWLEDGMENTS

We acknowledge fruitful discussions with Johan Carlström, Karl Sellin, Daniel Weston, and especially with J. M. Speight. This work is supported by the Swedish Research Council, by the Knut and Alice Wallenberg Foundation through the Royal Swedish Academy of Sciences fellowship, and by NSF CAREER Award No. DMR-0955902. The computations were performed on resources provided by the Swedish National Infrastructure for Computing (SNIC) at National Supercomputer Center at Linköping, Sweden.

APPENDIX A: ADDITIONAL MATERIAL

In Figs. 7 and 8, we give additional single flux quantum skyrmions for different values of the parameters of the interacting potential (5). In particular, we investigate here the role of $m = |\psi_1|^2/|\psi_2|^2$ parametrizing the relative ground-state densities of both charged condensates.

APPENDIX B: FINITE-ELEMENT ENERGY MINIMIZATION

We consider the two-dimensional problem (4) defined on a domain $\Omega \subset \mathbb{R}^2$ bounded by $\partial\Omega$. In our simulations, we choose the domain Ω to be a disk. The problem is supplemented by the boundary condition $\boldsymbol{n} \cdot \mathbf{D}\psi_a = 0$ with $\boldsymbol{n}$ the normal outgoing vector on $\partial\Omega$. This condition physically implies that no current flows through the boundary. This is thus a superconductor/insulator or superconductor/vacuum

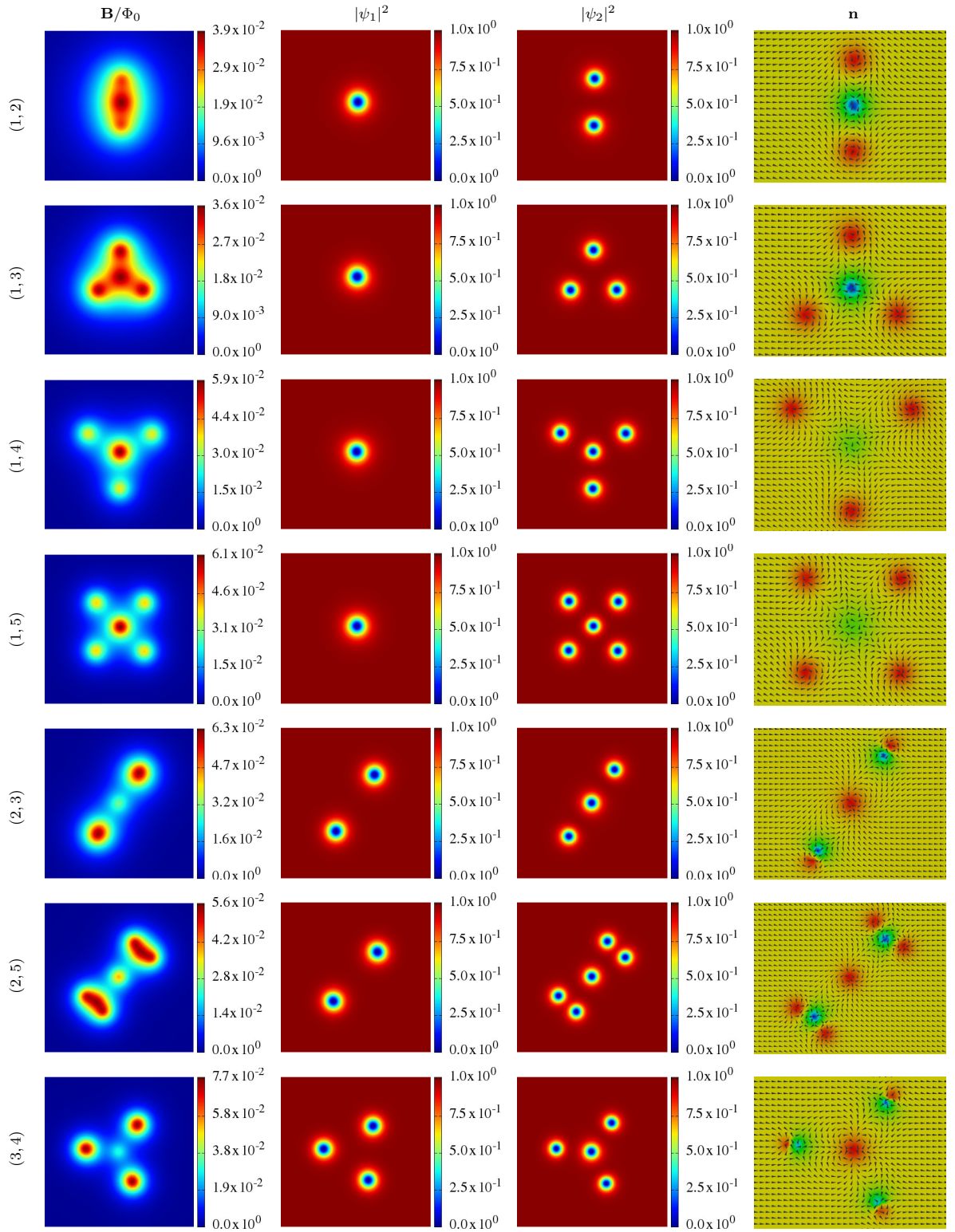

FIG. 7. (Color online) Single flux quantum topological excitations with disparity in the densities of each condensate. Here, the parameters of the Ginzburg-Landau functional (4) are $(\alpha_1,\beta_1) = (-3,1)$, $(\alpha_2,\beta_2) = (-5,5)$, and $e = 0.2$. Each row displays solutions for different winding parameters (g_1,g_2) (indicated on left). Displayed quantities in each row are respectively the magnetic field **B** (divided by the flux quantum Φ_0) and the densities of both condensates $|\psi_1|^2$ and $|\psi_2|^2$ (in units of their ground-state value). The rightmost panel displays the normalized projection of **n** onto the plane, while the color scheme indicates the magnitude of n_z. Blue corresponds to the south pole (-1) while red is the north pole $(+1)$ of the target sphere S^2.

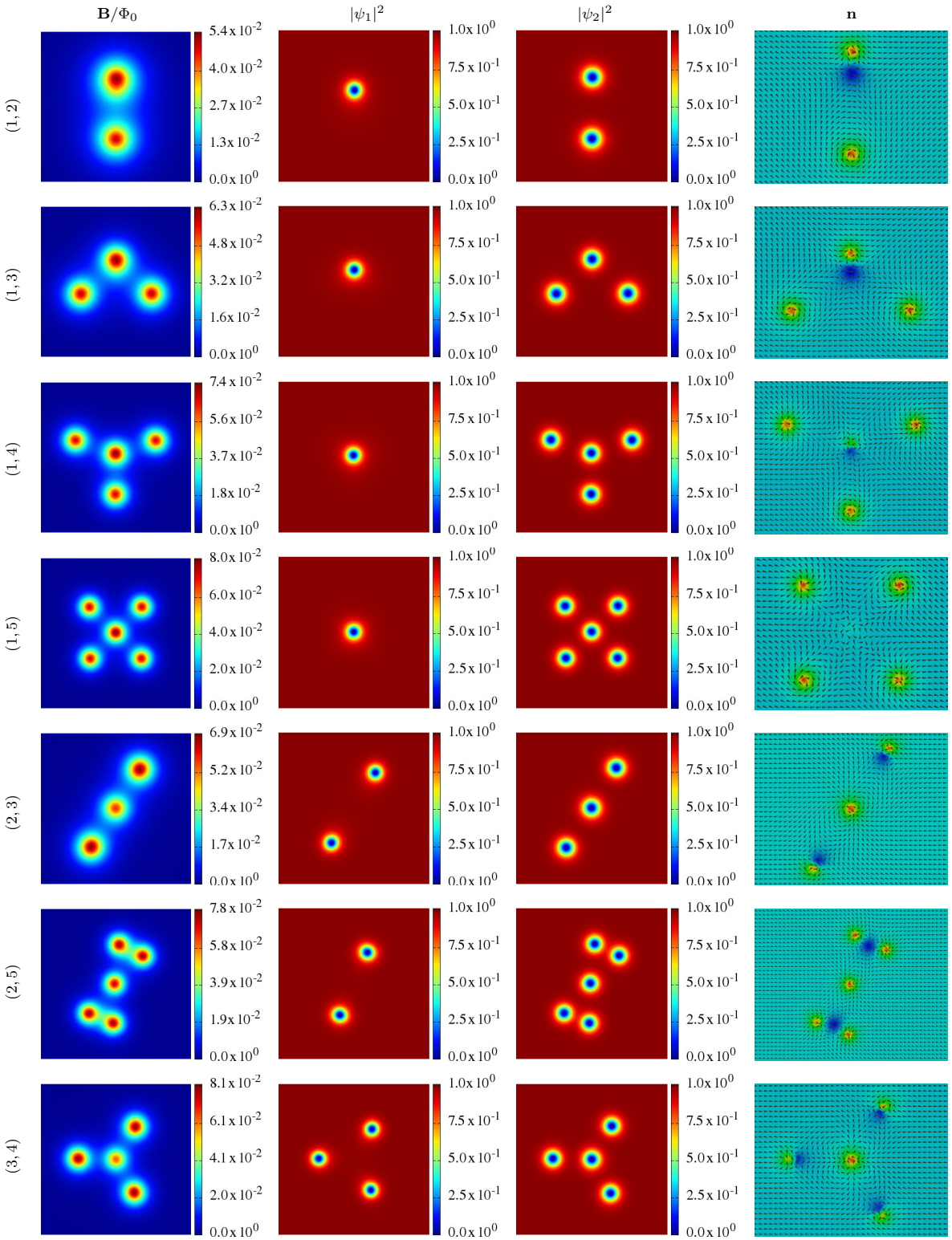

FIG. 8. (Color online) Vortex solutions carrying a single flux quantum. The parameters of the Ginzburg-Landau functional (4) are $(\alpha_1,\beta_1) = (-5,5)$, $(\alpha_2,\beta_2) = (-3,1)$, and $e = 0.2$. Each row displays solutions for different winding parameters (g_1,g_2) (indicated on left). Displayed quantities in each row are respectively the magnetic field **B** (divided by the flux quantum Φ_0) and the densities of both condensates $|\psi_1|^2$ and $|\psi_2|^2$ (in units of their ground-state value). The rightmost panel displays the normalized projection of **n** onto the plane, while color scheme indicates the magnitude of n_z. Blue corresponds to the south pole (-1) while red is the north pole $(+1)$ of the target sphere S^2.

boundary condition. Since this boundary condition is gauge invariant, additional constraint can be chosen on the boundary to fix the gauge. Our choice is to impose the radial gauge on the boundary $\boldsymbol{e}_\rho \cdot \mathbf{A} = 0$ (note that with our choice of domain, this is equivalent to $\boldsymbol{n} \cdot \mathbf{A} = 0$). This choice eliminates (most of) the gauge degrees and the boundary condition separates into two parts:

$$\boldsymbol{n} \cdot \nabla \psi_a = 0 \quad \text{and} \quad \boldsymbol{n} \cdot \mathbf{A} = 0. \tag{B1}$$

Note that these boundary conditions allow a topological defect to escape from the domain. To prevent this in simulations of individual skyrmions or skyrmion groups when no field is applied, the numerical grid is chosen to be large enough so that the attractive interaction with the boundaries is negligible. The size of the domain is then much larger than the typical interaction length scales. Thus, with this method one has to use large numerical grids, which is computationally demanding. This guarantees that the solutions are not boundary pressure artifacts. In particular this means that the observed core splitting cannot be attributed to finite-size effects as in mesoscopic samples [29–31].

The variational problem is defined for numerical computation using a finite-element formulation provided by the FREEFEM++ library [18]. Discretization within finite-element formulation is done via a (homogeneous) triangulation over Ω, based on the Delaunay-Voronoi algorithm. Functions are decomposed on a continuous piecewise quadratic basis on each triangle. The accuracy of such method is controlled through the number of triangles (we typically used $3 \sim 6 \times 10^4$), the order of expansion of the basis on each triangle (second-order polynomial basis on each triangle), and also the order of the quadrature formula to compute the integral on the triangles.

Initial guess

The initial field configuration carrying N flux quanta is prepared by using an ansatz which imposes phase windings around spatially separated $N_a = N g_a$ vortices in each condensate:

$$\psi_a = |\psi_a| e^{i\Theta_a + i\bar{\varphi}_a},$$

$$|\psi_a| = u_a \prod_{k=1}^{N_a} \sqrt{\frac{1}{2}\left[1 + \tanh\left(\frac{4}{\xi_a}\left[\mathcal{R}_k^a(x,y) - \xi_a\right]\right)\right]}, \tag{B2}$$

where $a = 1,2$, $u_a = \sqrt{-\alpha_a/\beta_a}$ is the ground-state density of a given condensate, and $\bar{\varphi}_a$ its ground-state phase. Because of $U(1) \times U(1)$ invariance, both $\bar{\varphi}_a$ can be chosen to be zero. ξ_a parametrizes the size of cores while the functions

$$\Theta_a(x,y) = \sum_{k=1}^{N_a} \tan^{-1}\left(\frac{y - y_k^a}{x - x_k^a}\right),$$
$$\mathcal{R}_k^a(x,y) = \sqrt{\left(x - x_k^a\right)^2 + \left(y - y_k^a\right)^2}. \tag{B3}$$

(x_k^a, y_k^a) denotes the position of the singularity of the kth vortex of the a condensate. The starting configuration of the vector potential is determined by solving numerically Ampère's equation on the background of the superconducting condensates given by Eqs. (B2) and (B3).

For a given starting configuration, the free energy is then minimized with respect to all degrees of freedom, with the condition (B1) that no current flows through the boundary. Here we used a nonlinear conjugate gradient method. The algorithm was iterated until relative variation of the norm of the gradient of the functional $\mathcal{F}$ with respect to all degrees of freedom was less than 10^{-6}.

[1] E. V. Herland, E. Babaev, and A. Sudbø, Phys. Rev. B **82**, 134511 (2010).
[2] E. Babaev, A. Sudbø, and N. W. Ashcroft, Nature (London) **431**, 666 (2004).
[3] E. Babaev and N. W. Ashcroft, Nat. Phys. **3**, 530 (2007).
[4] J. Oliva and N. W. Ashcroft, Phys. Rev. B **30**, 1326 (1984).
[5] J. Oliva and N. W. Ashcroft, Phys. Rev. B **30**, 5140 (1984).
[6] P. F. Bedaque, M. I. Buchoff, and A. Cherman, J. High Energy Phys. 04 (2011) 094.
[7] M. I. Eremets and I. A. Troyan, Nat. Mater. **10**, 927 (2011).
[8] D. Banerjee, M. Dalmonte, M. Müller, E. Rico, P. Stebler, U.-J. Wiese, and P. Zoller, Phys. Rev. Lett. **109**, 175302 (2012).
[9] E. Zohar, J. I. Cirac, and B. Reznik, Phys. Rev. Lett. **109**, 125302 (2012).
[10] E. Babaev, Nucl. Phys. B **686**, 397 (2004).
[11] A. B. Kuklov and B. V. Svistunov, Phys. Rev. Lett. **90**, 100401 (2003).
[12] E. Smørgrav, E. Babaev, J. Smiseth, and A. Sudbø, Phys. Rev. Lett. **95**, 135301 (2005).
[13] D. F. Agterberg and H. Tsunetsugu, Nat. Phys. **4**, 639 (2008).
[14] E. Berg, E. Fradkin, and S. A. Kivelson, Nat. Phys. **5**, 830 (2009).
[15] E.-G. Moon, Phys. Rev. B **85**, 245123 (2012).
[16] S. Sachdev, Nat. Phys. **4**, 173 (2008).
[17] K. Chen, Y. Huang, Y. Deng, A. B. Kuklov, N. V. Prokof'ev, and B. V. Svistunov, Phys. Rev. Lett. **110**, 185701 (2013).
[18] F. Hecht, J. Numer. Math. **20**, 251 (2012).
[19] E. Babaev, Phys. Rev. Lett. **89**, 067001 (2002).
[20] A reservation should however be made here. Mesoscopic systems, because they introduce a boundary cutoff on the divergent mode, can allow fractional vortices to be thermodynamically stable [29–31]. Also fractional vortices can also be thermodynamically stable near boundaries [32]. In our paper we however only consider bulk systems. In particular the simulation grid is chosen to be much larger than the size of vortices and thus boundary effects are irrelevant.
[21] Note that this physics of split vortices is entirely different from that of spatially separated fractional vortices that may also exist in different systems due to biquadratic density-density interaction [33,34,35], dissipationless drag interaction [24,36], or coexistence of vortices and domain walls [37,38]. In the case of mixtures of condensates with commensurate charges, the splitting occurs because of competing attractive interaction through the neutral sector and repulsive interaction mediated by the magnetic field. As discussed below, unlike for core splitting

induced by biquadratic terms, this physics is well captured in the London limit.

[22] E. Babaev, L. D. Faddeev, and A. J. Niemi, Phys. Rev. B **65**, 100512(R) (2002).

[23] E. Babaev, Phys. Rev. B **79**, 104506 (2009).

[24] J. Garaud, K. A. H. Sellin, J. Jäykkä, and E. Babaev, Phys. Rev. B **89**, 104508 (2014).

[25] J. Smiseth, E. Smørgrav, E. Babaev, and A. Sudbø, Phys. Rev. B **71**, 214509 (2005).

[26] P. Bonderson, V. Gurarie, and C. Nayak, Phys. Rev. B **83**, 075303 (2011).

[27] E. V. Herland, E. Babaev, P. Bonderson, V. Gurarie, C. Nayak, and A. Sudbø, Phys. Rev. B **85**, 024520 (2012).

[28] E. V. Herland, E. Babaev, P. Bonderson, V. Gurarie, C. Nayak, L. Radzihovsky, and A. Sudbø, Phys. Rev. B **87**, 075117 (2013).

[29] L. F. Chibotaru, V. H. Dao, and A. Ceulemans, Europhys. Lett. **78**, 47001 (2007).

[30] R. Geurts, M. V. Milosevic, and F. M. Peeters, Phys. Rev. A **78**, 053610 (2008).

[31] L. F. Chibotaru and V. H. Dao, Phys. Rev. B **81**, 020502 (2010).

[32] M. A. Silaev, Phys. Rev. B **83**, 144519 (2011).

[33] M. Nitta, M. Eto, and M. Cipriani, J. Low Temp. Phys. **175**, 177 (2014).

[34] M. Kobayashi and M. Nitta, J. Low Temp. Phys. **175**, 208 (2014).

[35] D. F. Agterberg, E. Babaev, and J. Garaud, arXiv:1403.6655.

[36] S. B. Chung, H. Bluhm, and E.-A. Kim, Phys. Rev. Lett. **99**, 197002 (2007).

[37] J. Garaud, J. Carlström, E. Babaev, and M. Speight, Phys. Rev. B **87**, 014507 (2013).

[38] J. Garaud, J. Carlström, and E. Babaev, Phys. Rev. Lett. **107**, 197001 (2011).